2012 International Conference on Indoor Positioning and Indoor Navigation, 13-15th November 2012

Automatic 3D Calibration for a Multi-Sensor System

The concept of a 3D calibration method of a radio-based Multi-Sensor System for Indoor Localisation

Enrico Köppe
Division 8.1 Sensors, Measurement and Testing Methods
BAM, Federal Institute for Materials Research and Testing,
Berlin, Germany
enrico.koeppe@bam.de

Daniel Augustin, Achim Liers, Jochen Schiller
FU Berlin,Computer Systems &Telematics
Berlin, Germany
Daniel.Augustin, Achim.Liers, Jochen.Schiller@fu-berlin.de

***Abstract*—A major current focus in multi-sensor systems for indoor localisation is how to calibrate the sensors. In this study, we introduce a new method for this task. By using the datafusion of the combined sensor data, we were able to eliminate the errors of an individual sensor. The challenging matter was the connection of the different sensors for a continuous calibration. The necessary data for the calibration were given due to the natural movement of a person. The examination of this values offers an automatic re-calibration without using a given calibration sequence. This finding is promising for improving the calculation of the exact position of a person, who is moving free in a room.**

Keywords—wireless sensor network (WSN); embedded systems; sensor calibration and validation; person tracking; inertial navigation system; inertial measurement unit; indoor localisation

I. INTRODUCTION

Generally, the sensors (3D accelerometer, 3D gyroscope, 2D compass sensor and 3D magnetic field sensor) are calibrated using a defined movement in a room (3D) or on a surface (2D). There are two most commonly used methods to establish the reference data which is the geomagnetic field and gravity acceleration for the different sensors. The first method is based on the virtual motion of the sensors on a horizontal eight to determine all local magnetic field lines [1] and the acceleration maximum of 1 g respectively of -1 g [2]. The second method uses a slow, non-directional motion around all axes in the room for the determination of the acceleration maximum. Slightly problematic of these methods is the definition of the motion. This has to be done before the calibration and the test starts. Consequently, this calibration depends on the actual position of the system. That means we receive a place dependent parameter for the reference data. Once a sensor is calibrated, it is difficult to execute a spontaneous recalibration due to ad-hoc influences such as a temperature based error or magnetic offset.

With the knowledge of this problem a new principle was implemented for the calibration method. This principle is based on the free motion at the curved surface area of an ellipsoid which allows free motion calibration of the sensor at any place or position. In the same way the algorithm can use the movement of the holder as input for a continuous recalibration during a normal operation.

By moving the sensor system in a pseudo static motion, measurement data is generated and used to determine the ellipsoid. This geometrical figure describes the sensor idle state and amplitude at a known measurement value. The algorithm, implemented uses an optimisation algorithm to gain the ellipsoid out of noisy measurements. Furthermore, the advantage of this principle is that it is possible to calibrate a free motion of the sensor system at any place or position on a person. In other words the sensor system is calibrated and adjusted during normal operation. Hence, there are no more movements after the activation of the system or during the working process necessary for the calibration [3].

II. THEORIE OF OPERATION

The calibration method is based on the assumption that every detected value of a 3D sensor is on the curved surface area of a sphere. Therefore, the existing error of the sensor and the asymmetry of the individual sensors are neglected. Consequently the centre of the assumed sphere describes the rest position of the sensor. The radius r of the sphere is the displacement at known field intensity, for example 1g. Furthermore, this principle of a curved surface area only works for systems with superior reference system, e.g. gravity and magnetic field of the earth. Another restriction is the error in the shape of the curved surface area (ellipsoid versus sphere) which is caused by the executed approximations. In the first approximation the sensors have a measurement error causing a noisy scatter-plot around the curved surface area of the sphere. In the second approximation there is no symmetry of the sensor axles which refers to the real case. The reason for the absent symmetry is the differing scale at the AD-compilation or the distortion of the emitted field. In short the approximations are responsible for the evolution of an ellipsoid from the scatter-plot of the sensor values.

A. The ideal model

Theoretically, the ideal model is a good assumption taking into account an ideal, error-free sensor which reproduces the environmental data undistorted as magnetic field lines. The measured sensor data are located on the curved surface area

precisely. Thus the sum of all discrepancies of the sphere model is always zero. In this case four linear independent measured values are enough to determine a unique sphere. Figure 1 shows the position of the measured values of the sphere model in the ideal case. In practical work this ideal model does not fit.

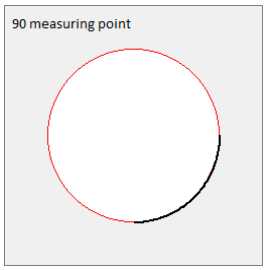

Figure 1. Ideal measurement area, all values are on the curved surface area of a sphere.

B. *The symmetric model*

The most common method in practice is the symmetric model on account of its simplicity. This model uses the mathematical method of least squares to determine the values. It is based on the assumption of a normal distribution of the measurement error which can be seen as scatter-plot with a radius $r$around the curved surface area. In Figure 2 the distribution of the measured values is shown.

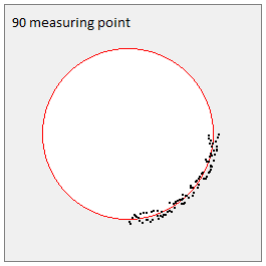

Figure 2. Symmetric measurement area, mapping of a pointcloud on the curved surface area of an ellipsoidwith $r = r_x = r_y = r_z$.

C. *The asymmetric (real) model*

In addition to the symmetric model the number of degrees of freedom is increased in the asymmetric model. Therefore the radius r is splitted in the radius of the axes r_x, r_y, r_z. On the basis of this model scaling errors of the calibration were taken into account of the different axes of the sensors or of the distortions in the measured fields. This leads to the optimisation of the determination of the position. Above all asymmetric errors can be constructive single component faults or temperature influences in the process.

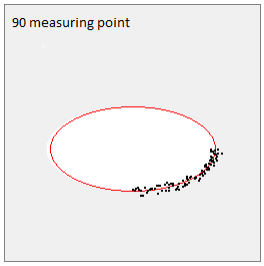

Figure 3. Asymmetric model, mapping of a pointcloud of the curved surface area of an ellipsoid wirh $r_x \neq r_y \neq r_z$.

D. *Determination of the model parameters*

The method of the least squares is used for the squared deviation of the measured values of the curved surface area of an estimated sphere [4], [5]. Due to iteration over the measured values the sphere parameters were adjusted as long as there is no improvement of the possible squared total error. The iteration process ends in a minimum which is not necessarily the optimum selection of the parameters. On account of additional local minima there are other optimum selections of the parameters for these local areas.

$$f(x, y, z, x_0, y_0, z_0, r) = (x - x_0)^2 + (y - y_0)^2 + (z - z_0)^2 - r^2 \quad (1)$$

The function in equation (1) determines the squared gap of a point P(x,y,z) relating to the curved surface of a sphere (x_0, y_0, z_0, r). If the point P is on the curved surface area of the sphere then the function f(x, y, z, x_0, y_0, z_0, r) in (1) is going to be zero.

$$E = \sum_{i=1}^{n} (f(x_i, y_i, z_i, x_0, y_0, z_0, r))^2 \quad (2)$$

To calculate the squared errors over all points of a measurement series the function in equation (2) is used. The errors of the sphere (x_0, y_0, z_0, r) are investigated as the sum of the single square. The method of the least squares approximates the sphere parameters so that the squared total error is minimal (3).

$$\min_{f(x,y,z,x_0,y_0,z_0,r)} E \quad (3)$$

Due to a minimal radius as a constraint, the search for all minima is possible. The calibration process terminates for every radius r_{min} in a local minimum with $r \geq r_{min}$. However, the optimum selection of the parameters is given by the minimum with the smallest total error. In Figure 4 is shown how the smallest radius increases stepwise during the approximation of a circle. Little by little you can see the minima which reduce the total error on the smaller previous minimum.

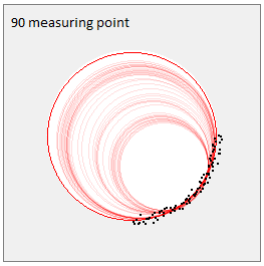

Figure 4. Determination of the best minima to optimise the calibration error.

III. Experimentel Setup

Our study approaches a continuous and exact calibration process on the basis of the natural movement of a human being. For this reason a small movement will be approximated on a whole sphere surface to avoid a complex calibration setup and process. In that case the necessary movements for the determination of the calibration values are reached by the simple motion of the wrist about ± 15°. The used sensors for the application and examination of our method are the analogue 3D acceleration sensor MMA7260 (Freescale, USA) and the digital 3D acceleration sensor LSM303DLH (ST, USA). This last sensorLSM303DLHhas an additional integrated3D magnetic field sensor, which is used for our calibration. Another sensor used for the calibration respectively the determination of the magnetic field is the 2D compass module HMC6352 (Honeywell, USA). Furthermore, to determine the rotation the analogue 1D gyroscope EMC-03R (Murata, Japan) and the analogue 1D gyroscope LY330ALH (ST, USA) are used. Additionally, the analogue 2D gyroscope LPR430AL (ST, USA) is utilised. The measurement points of the different sensors are read out and digitised at a measurement frequency of 100 Hz, except the HMC6352 who was read out at 10 Hz.

All mentioned sensors are integrated in two different working systems. The sensors (MMA7260, HMC6352, EMC-03R) are inserted in the Bodyguard-System [6] and the sensors

978-1-4673-1954-6/12/$31.00 ©2012 IEEE

(LSM303DLH, LY330ALH, LPR430AL) are inserted in the iNEMO [7].

To compare different approaches on experimental basis, all measurements have been recorded to file. Each recording contained a round 5000-20000 datasets.

The stability of the sphere approximation was analysed by raising the set of considered measurements step by step. It also gives a picture on how fast the algorithm reaches a stable state at which additional measurements do no longer appreciably manipulate the parameters of the approximated sphere.

Having an estimation of the minimal needed number of measurements, the given dataset is split into smaller sets on which the algorithm is tested repeatedly. The results have been used to check equality of the parameters based on different calibration routines.

The algorithm was optimized with regard to speed and stability, checking different optimizing mechanisms and pre-filtering algorithms with empiric determination of parameters. Aiming at an algorithm that runs on the sensor platform, not all promising approaches have been useable because of ambitious demands of computing capacity. Especially in consideration of realising a continuous calibration of the magnetometer, those results have been taken seriously, which have been fast but less accurate. Unlike a single calibration routine, a continuous one allows to include real-time results in terms of evaluating the precision of a single calibration step.

Figure 5. Software for the determination of the measured values, Visualisation of the radius and of the resulting calibration value during a free motion around the wrist using the Bodyguard-System.

IV. RESULTS

At the start of the calibration method the measured values, covering the curved surface area, are used to approximate the sphere model. Next, the quality of the first approximation is analysed by increasing this covered curved surface area stepwise.

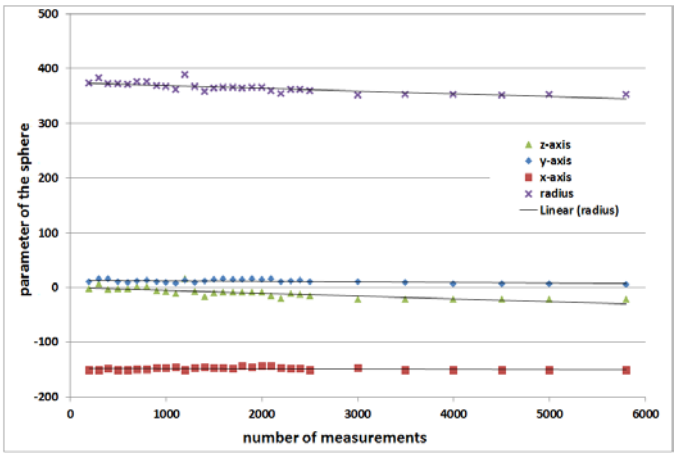

Figure 6. Approximation of the sphere surface due to small movements till 200 measurements and from 2500 measurements bigger movements were made.

Due to conscious rotation about the single axes more entire circles are enforced on the curved surface. A better way of putting it is to say the more information on the curved surface area is collected the merrier are the circles which approximate this curved surface area. Accordingly, using the number of measured values and the approximated sphere models, conclusions can be made about the quality of the calibration during a free natural movement. In Figure 6 the curve of the parameters of an approximated sphere over the number of measurements is shown. In the range of 200 till 2500 measurements the movements of the wrist are small, but from 2500 measurements there is a whole rotation of the wrist. As you can see in figure 6 the curves are horizontal that means the single parameters are logic even though using an approximation of few measurement points at the higher number of measurements (from 2500 only a few points for the approximation). For all calculated sphere parameters the behaviour of value x_0 is most constant with a standard derivation of 1.71. Due to construction design the z-axis has a higher error, which leads to a noisy calibration result with a standard derivation of 9.34. It also degrades the stability of the approximated radius which leads to a standard derivation of 9.72 for that value.

TABLE I. STANDARD DEVIATION OF THE SPHERE BASED ON MAGNETOMETER MEASURMENTS

Number of measurments	Parameter of the sphere			
	x_0	y_0	z_0	r
5800	-150	6	-21	352
5000	-151	7	-21	353
4500	-151	7	-23	351
4000	-151	7	-22	353
3500	-151	9	-21	353
3000	-147	10	-23	351
2500	-151	10	-16	359
2000	-143	14	-9	365
1500	-147	14	-11	364
1000	-147	9	-7	367
900	-147	10	-6	368
800	-149	13	1	376

Number of measurments	Parameter of the sphere			
	x_0	y_0	z_0	r
700	-149	11	1	375
600	-151	9	-3	371
500	-151	10	-2	372
400	-148	15	-4	372
300	-150	15	7	383
200	-150	10	-2	373
Standard deviation	**1,71**	**2,47**	**9,34**	**9,72**

However, the experimental data for the calibration of the sensors was smoothed due to a Kalman filter. Although the empirical variance of the single measured values was expected as a uniformly distributed measurement error. Nevertheless a correction or a plausibility test of the single measured values was not done.

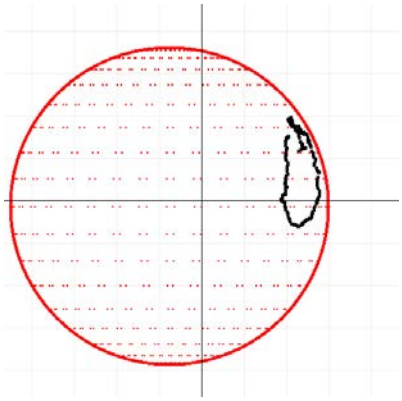

Figure 7. Visualisation of the calibration with 200 measurement values at a short rotation of the wrist.

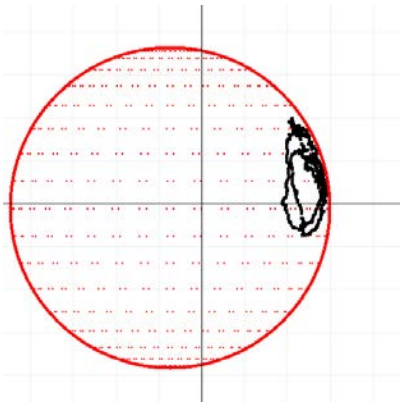

Figure 8. Visualisation of the calibration using 1000 measurement values and a rotation of the sensor system about 45°.

The movements in figure 7 and 8 show a small rotation of the wrist. These correspond to a measured movement from a system which is connected to the hip loosely. During this motion the calculated radius of the curved surface area deviates about 6%. If the multi-sensor system is still moving with small rotations with increasing time the deviation of the radius is reduced to only 2%. However, if there are bigger rotations of the wrist as shown in figure 9 the measured error is under 1%.

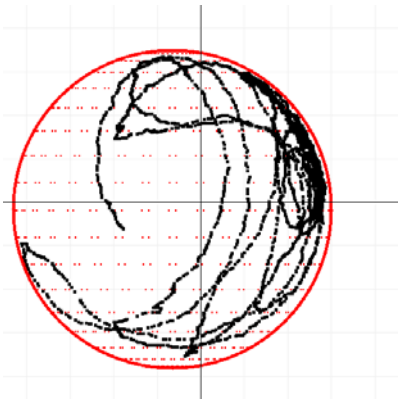

Figure 9. Visualisation of the calibration with 3500 measurement values and a lot of complete rotations.

But this low error of less than 1% only occurs by using long-standing measurement series. The real error respectively the standard deviation of all measurements is at 9.72. Therefore the good results must be relativised. We suppose a low standard deviation due to the knowledge of the possibility to correct the measurement values backward on account of the automatic continuous calibration. But this must be confirmed conducting further investigations.

Further, in the next three figures the calculation of the function of an ellipsoid is shown. The calculation is almost the same as the „hard iron offset"-calculation for magnetic fields [8], [9]. In our method the radii form the acceleration [4], the angular velocity and the rest position of the system using the magnetic field of the earth.

Initially the measured data are recorded which is shown for a scatter-plot in figure 10.

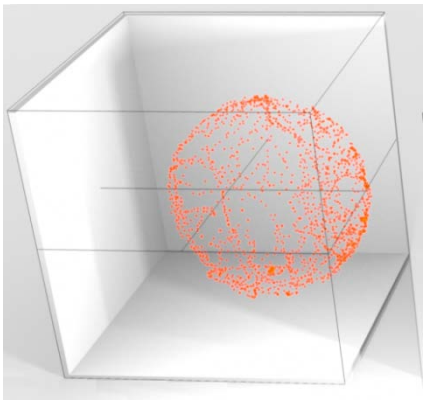

Figure 10. First step for the calculation of the function of an ellipsoid with a scatter-plot due to a continous motion.

As soon as the measurement values are recorded the volume of the sphere is calculated by the approximation of the least squares. Next the sphere is stepwise increased till the shape of an ellipsoid is almost reached („fitting volume"). In figure 11 the calculated ellipsoid of the measured scatter-plot is shown consisting of a lot of single ellipses [10], [11].

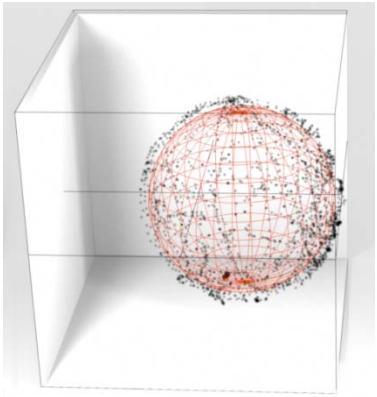

Figure 11. Second step for the calculation of the function of an ellipsoid: Search for the “fitting volume”due to the approximation of the least squares.

Finally we search for the centre of the ellipsoid which is approximated using the “fitting volume” function [12]. Nevertheless, this centre is the gravity centre of the ellipsoid and displays the rest position of the sensor system.

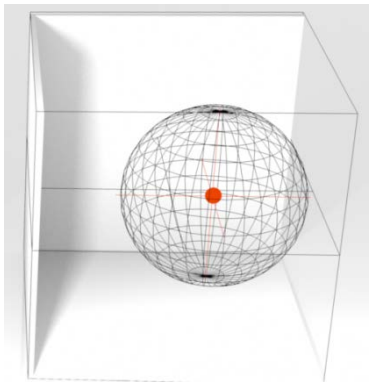

Figure 12. Final step for the calculation of the fuction of an ellipsoid:The centre equatesto th radius of the ellipses or the ellipsoid.

At the moment the method for the calculation of the gravity centre is realized using the PC. In the future this will be done using the microcontroller of the Bodyguard-System [6]. Thus is necessary to improve the indoor and outdoor localization of the person.

In the realised experiments the determined scatter-plots are mapped on the sphere surface as approximation of the least squares. Consecutively, the approach to the sphere surface and the projection of the single axles are shown in the following figures.

At first we look at the approach of the acceleration sensor to the circle surface in figure 13.The values for the single axles are given with r_x = 1048, r_y = 998 and r_z = 1064.This radii match with the calibration value of 1 g of the gravity acceleration of each axis.

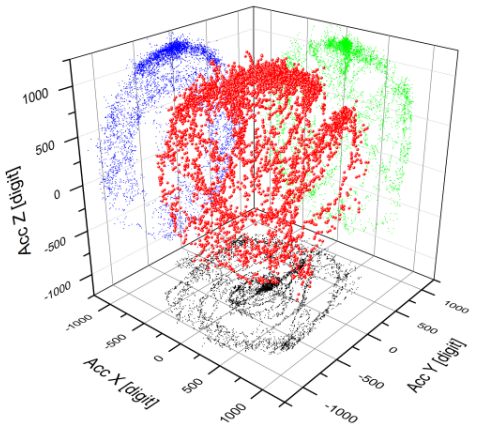

Figure 13. Ellipsoid of the acceleration sensors as function of the acceleration.

Next, calculating the curved surface area of the gyroscope, the map is not that clear as the one of the acceleration sensor because of the reproduction of the curved surface area by the relative movement as velocity. If we transfer the angular change to the angular velocity the curved surface area can be mapped. The radius of the curved surface area of the used gyroscope is r_{pitch} = 69, r_{roll} = 65 and r_{yaw}= 250.

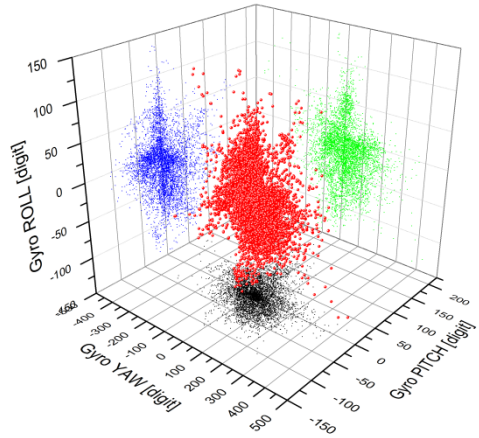

Figure 14. Ellipsoid of the gyroscope as function of the angular velocity.

At last the magnetic field sensor is mapped and shown in figure 15. If we use an approximation of the radii of the magnetic field sensor the transfer to the curved surface area is definite. The determined radii of the curved surface area are influenced by external magnetic fields. Hence there are problems with the “hard iron offset” and the “soft iron offset”. These problems are solved using software for the extrapolation of the radii. Now the values for the mapping of the magnetic field sensor can be given with the radii of the curved surface area r_x = 248, $r_{xOffset}$ = -100, r_y = 328 and r_z = 356.

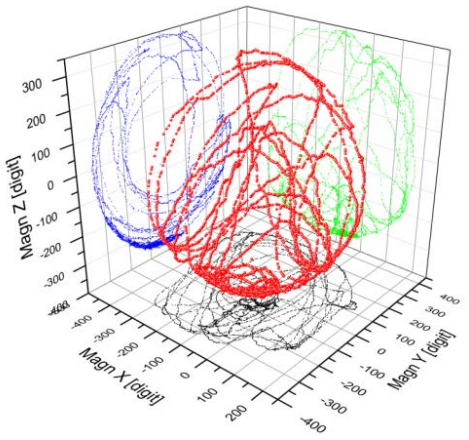

Figure 15. Ellipsoid of a magnetic field sensor as function of the magnetic field of the earth.

V. CONCLUSION AND OUTLOOK

Our method verifies an improvement of the determination of a position from an error of 3% with a singular mechanical calibration [3] to an error of 1.5 – 2% with the automatic calibration during the initiation of the system respectively during the system is running. For comparison, the error without calibration is around 10%. Besides there is an additional improvement of the results possible due to a readjustment or a plausibility test of the single measured values. Furthermore, the quality of the calibration can be improved using the grouping of close to each other lying measurement points and using the filtering of outliers (RANSAC algorithm [13]).

At the moment the described algorithm is realized at the PC. For the determination of the rest position and the calibration values of the single sensors, independent of their size and deformation on the Bodyguard-System, the algorithm will be imported in the software of the Bodyguard-System in the future. This calculation on the Bodyguard-System simplifies the processing of the normed sensor data in a new position in the software on the PC. So it is no longer necessary that the PC knows the rest position and the calibration values. Hence the determination of the position of a person is faster and easier on the PC.

To sum up, the position error of a particular position can be reduced to below 2 % due to the automatic calibration of the sensors when activating the system. Hence it is possible to determine the exact position of a person in a building.

[1] WELLS Counter Point, Understanding Hall Effect Sensors http://www.wellsve.com/sft503/Counterpoint3_1.pdf

[2] Texas Instruments, Accelerometers and how they work http://www2.usfirst.org/2005comp/Manuals/Acceler1.pdf

[3] Enrico Köppe (2011), IPIN 2011, Tracking Persons with a Radio-Based Multi-Sensor System, http://ipin2011.dsi.uminho.pt/PDFs/Shortpaper/100_Short_Paper.pdf

[4] Bradley Nevins Damazo, Mechanical, Sensor and Control System Design for an Accelerometer Calibrator with One Part per Million Accuracy

[5] Gilbert Strang (2009), Introduction to Linear Algebra 4.3 - Least Squares Approximations http://math.mit.edu/linearalgebra/ila0403.pdf

[6] Enrico Köppe (2012), Radio-based multi-sensor system for person tracking and indoor positioning, WPNC 12, pp 180- 186

[7] STMicroelectronics, INEMO, iNEMO system-on-board (2012), http://www.st.com/internet/com/TECHNICAL_RESOURCES/TECHNICAL_LITERATURE/DATA_BRIEF/DM00046903.pdf

[8] MEDER electronic, Sensor vs. Hall Effect http://www.meder.com/fileadmin/meder/pdf/en/Technical_Documents/Reed_Sensors_vs._Hall_Effect_Sensors.pdf

[9] Oscar Sandoval Gonzalez, Hall Effect Sensors http://sandoval-gonzalez.com/5_hall.pdf http://dspace.mit.edu/bitstream/handle/1721.1/33474/19088040.pdf

[10] Eero P. Simoncelli (2012), Least Squares Optimization http://www.cns.nyu.edu/~eero/NOTES/leastSquares.pdf

[11] Walter Ganter, Gene H. Golub, Rolf Strebel Least-Squares Fitting of Circles and Ellipses http://www.ulb.ac.be/assoc/bms/Bulletin/sup962/gander.pdf

[12] Britta Nestler, Modellierung und Simulation, Ausgleichsproblem http://www.iam.kit.edu/zbs/download/ModSim-Skript3.pdf

[13] RANSAC for Dummies (2012), Marco Zuliani, http://vision.ece.ucsb.edu/~zuliani/Research/RANSAC/docs/RANSAC4Dummies.pdf